

# Decaying dark matter: a stacking analysis of galaxy clusters to improve on current limits

C. Combet\* and D. Maurin

*Laboratoire de Physique Subatomique et de Cosmologie,  
Université Joseph Fourier Grenoble 1/CNRS/IN2P3/INPG, 53 avenue des Martyrs, 38026 Grenoble, France*

E. Nezri

*Laboratoire d'Astrophysique de Marseille - LAM, Université d'Aix-Marseille & CNRS,  
UMR7326, 38 rue F. Joliot-Curie, 13388 Marseille Cedex 13, France*

E. Pointecouteau

*(1) Université de Toulouse (UPS-OMP), Institut de Recherche en Astrophysique et Planetologie  
(2) CNRS, UMR 5277, 9 Av. colonel Roche, BP 44346, F 31028 Toulouse cedex 4, France*

J. A. Hinton and R. White

*Dept. of Physics and Astronomy, University of Leicester, Leicester, LE1 7RH, UK*

(Dated: October 11, 2018)

We show that a stacking approach to galaxy clusters can improve current limits on decaying dark matter by a factor  $\gtrsim 5 - 100$ , with respect to a single source analysis, for all-sky instruments such as Fermi-LAT. Based on the largest sample of X-ray-selected galaxy clusters available to date (the MCXC meta-catalogue), we provide all the astrophysical information, in particular the astrophysical term for decaying dark matter, required to perform an analysis with current instruments.

PACS numbers: 95.35.+d, 98.65.-r

## I. INTRODUCTION

The nature of dark matter (DM) is one of the major questions in both modern astrophysics and fundamental physics. In the most popular extensions of the standard model, an explicit symmetry provides stable annihilating DM candidates. Nevertheless, decaying DM is an equally well-motivated scenario; it arises in several consistent extensions beyond the standard model. Among those candidates and frameworks, a non-exhaustive list includes: gravitinos in R-parity breaking models [1, 2], sterile neutrinos [3], hidden sector gauge bosons [4], hidden sector particles [5], right-handed neutrinos/sneutrinos [6], bound states of strongly interacting particles [7]. To be viable in the DM context, these models should induce a DM lifetime longer than the age of the universe.

For the case considered here (see below), the total flux expected from decay, in a given direction  $(l, b)$  (Galactic coordinates) and integrated over the solid angle  $\Delta\Omega$ , is given by the product of a particle physics term with an astrophysical term  $D$

$$\frac{d\phi(E, l, b, \Delta\Omega)}{dE} = \frac{dN}{dE}(E) \times D(l, b, \Delta\Omega). \quad (1)$$

Depending on the decaying DM candidate, the photon spectrum  $dN/dE$  can be a mono-energetic line (from  $\gamma\gamma$  and  $\gamma\nu$  channels), or a continuum (e.g., for some gravitino

candidates above a few hundred GeV [8]). The mass of the candidate can span a large range depending on the model. For this reason, a signal is generally searched for in X-rays [9, 10], or in  $\gamma$ -rays [11]. In the  $\gamma$ -ray regime, the most stringent limit on the DM lifetime (that arises in the spectral term) comes from the non-detection by the Fermi-LAT collaboration [12] of emission from the directions of galaxy clusters [13].

Here we focus on the astrophysical factor

$$D(l, b, \Delta\Omega) = \int_{\Delta\Omega} \int \rho(l', \Omega) dl' d\Omega, \quad (2)$$

which is the integral of the DM density,  $\rho(l', \Omega)$ , over line of sight  $l'$  and solid angle  $\Delta\Omega = 2\pi \cdot (1 - \cos(\alpha_{\text{int}}))$ , where  $\alpha_{\text{int}}$  is the integration angle. When  $D$  is computed over cosmological distances, the spatial term becomes coupled to the energy-dependent term as  $\gamma$ -rays are absorbed along the line of sight ( $e^{-\tau(E, z)}$  attenuation factor, see, e.g., [14]). ‘Cosmological’  $\gamma$ -rays will also be redshifted, affecting the spectrum. Here however, our analysis relies on the MCXC catalogue of galaxy clusters [15], the redshift distribution of which peaks at  $z \sim 0.1$  (see their Fig. 1) so that we can safely neglect the above processes. This allows us to factor out energy-dependent effects, i.e. the spectrum resulting from a prompt emission and also an inverse Compton (IC) contribution from scattered DM-induced electrons and positrons. The benefit is twofold: i) it simplifies the discussion, and ii) also avoids introducing strongly DM model-dependent factors. Note however, that the respective IC contributions in the Galaxy and in the clusters are probably different, and this should be kept in mind when comparing the Galactic DM diffuse

\*Electronic address: celine.combet@lpsc.in2p3.fr

and galaxy cluster  $D$ -factors.

As in the case of searches for annihilating DM, interesting targets include dwarf spheroidal galaxies, our own Galaxy, and clusters of galaxies [16]. Recently, diffuse  $\gamma$ -ray emission [14] and cross-constraints with other channels (e.g., anti-protons and positrons) have also been considered [17–21]. These studies rely on the analysis of single objects or small samples constituted by what are thought to be the best targets. As underlined in [8], one advantage of combining several galaxy clusters is that uncertainties (for example on the total mass and DM concentration) somewhat cancel out.

With this in mind, we show below how the astrophysical term  $D$  can be increased by a stacking strategy of galaxy clusters without compromising sensitivity due to increasing the amount of background integrated. For that purpose, we take advantage of the recently published Meta-Catalog of X-ray detected Clusters, MCXC [15], which encompasses 1743 clusters of galaxies (making it the largest sample of clusters with detected X-ray emission from their hot gas).

## II. METHOD

### A. Galactic and cluster signal

All calculations of the  $D$ -factor are performed with the public code *CLUMPY* v2011.09 [22]. The Galactic DM halo is chosen to follow an Einasto profile [23] with a local density  $\rho_{\odot} = 0.3 \text{ GeV cm}^{-3}$ . We assume that the DM profiles of all the galaxy clusters in the catalogue follow a NFW parametrisation [24]. For a cluster, we use the standard definition for  $R_{\Delta}$  to be the radius within which the average density reaches  $\Delta$  times the critical density of the Universe (at a given redshift). The mass  $M_{\Delta}$  is then simply the mass enclosed within  $R_{\Delta}$ . Most observational constraints and predictions are expressed in terms of  $\Delta = 500$  or  $\Delta = 200$ . Using values for  $M_{500}$  (derived from the X-ray luminosity) provided in the MCXC meta-catalogue [15], we use a mass-concentration relationship [25] to derive the scale radius and normalisation of the NFW profile for each cluster. To first order, the uncertainties related to X-ray observations (i.e.  $\sim 15\%$  average on  $M_{500}$ ), and the scatter related to the mass-concentration relationship [25] average out if the stacked signal from a large sample of clusters is considered.

### B. Extragalactic isotropic signal

As shown in [14], contrary to the DM annihilation case, the extra-galactic DM decay contribution is a robust quantity depending mostly on the mean DM density of the universe  $\Omega_{\text{DM}}\rho_{c,0}$ . For the sake of simplicity, we neglect the absorption  $\tau(E, z)$  as it has only a moderate impact below 100 GeV [14]. Doing so yields an upper

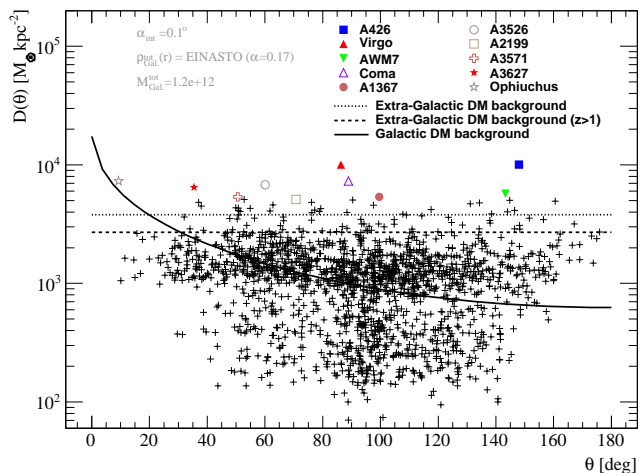


FIG. 1: Astrophysical factor for decaying DM. Symbols are for galaxy clusters, solid line is for the Galactic DM background, and the dotted and dashed lines are an upper-limit (no absorption on the extragalactic background light) for the isotropic extragalactic DM background (see Eq. 3). The 10 brightest objects are identified with coloured symbols.

limit for this contribution that is written as

$$D_{\text{extra-gal.}}^{\text{u.l.}}(\Delta\Omega, > z) = \Delta\Omega \int_z^\infty \frac{\Omega_{\text{DM}}\rho_{c,0}}{H(z')} dz', \quad (3)$$

where  $H$  is the Hubble constant for the concordant  $\Lambda$ -CDM cosmology. This quantity is used below for illustration purposes only, as a limit to the continuum signal which can drown the cluster signal (see in particular Section III B).

## III. RESULTS

Figure 1 shows the astrophysical term  $D$  (in  $M_{\odot} \text{ kpc}^{-2}$ ) for each cluster (plus symbols) as a function of its angle  $\theta$  w.r.t. the Galactic centre direction. A large number of objects outshine the Galactic DM background (the solid line), fewer outshine the extragalactic signal upper limit (dotted line). Being a compilation of various X-ray cluster catalogues, the MCXC meta-catalogue is not complete at any redshift or in any mass range. This diversity is reflected by the less populated region below the Galactic signal (solid line) in Fig. 1. In principle, an integration along  $z > 0$  of the extragalactic signal amounts to some double counting of the MCXC galaxy clusters. The dashed line calculated for  $z > 1$  illustrates how much this double counting could be at most (since the MCXC catalogue is not complete up to this redshift).

An integration angle of  $\alpha_{\text{int}} = 0.1^\circ$  is adopted, corresponding to the typical angular resolution of current  $\gamma$ -ray instruments well above threshold (e.g., Fermi-LAT for energies above  $\sim 10$  GeV, H.E.S.S. above  $\sim 300$  GeV). This choice is appropriate for the signal from cluster halos, as their typical angular scale (i.e.,  $R_{500}$ ) is  $0.1^\circ - 1^\circ$ .

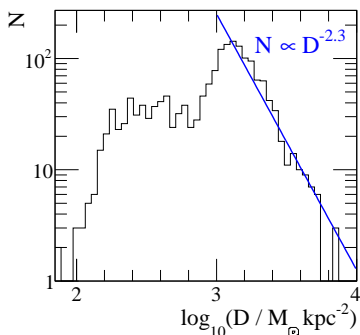


FIG. 2:  $\log N - \log D$  for the galaxy cluster population for  $\alpha_{\text{int}} = 0.1^\circ$ . The behaviour for the brightest objects is consistent with  $N \propto D^{-2.3}$ .

However, we underline that the Galactic and extragalactic signals scale with  $\alpha_{\text{int}}^2$ , so that smaller integration angles are in principle favoured to increase the contrast between the cluster signal and these DM backgrounds.

### A. $\log N - \log D$

The promise of a stacking analysis for decay is suggested from Fig. 2. The  $\log N - \log D$  plot has a slope of  $-2.3$  at large values of  $D$ : the number of objects increases faster than the signal decreases. The incompleteness of the MCXC meta-catalogue is seen as a drop for  $D < 10^3 M_\odot \text{ kpc}^{-2}$ . A larger and more complete catalogue with a well defined selection function could further increase the gain provided by a stacking approach if the  $N \propto D^{-2.3}$  behaviour continues down to smaller  $D$  values. In a few years from now, the eROSITA mission [26] should provide such a catalogue. There is naturally a limit to this gain, as at large redshift, clusters may not have formed yet. The maximum gain can in principle be estimated from the theoretical redshift distribution of clusters, or from the use of more complete, e.g. optical, galaxy cluster catalogues (although these observations poorly constrain the cluster DM content). For the current study we focus on X-ray identified clusters to reduce uncertainties in the DM signal and to provide a list of target objects to current observatories.

### B. Stacking

Figure 3 (upper panel) shows the cumulated signal of all galaxy clusters having an astrophysical factor  $> D$  as a function of  $D$ . In all cases the cumulative signal saturates at  $< 800$  clusters, consistent with the drop-out seen in Fig. 2. For the case of  $\alpha_{\text{int}} = 0.5^\circ$  (black circles) the integrated  $D$  for 791 clusters is  $6 \cdot 10^6 M_\odot \text{ kpc}^{-2}$ , a factor  $\sim 30$  above the value for the top two clusters (furthest right point). For each  $D$  bin, the corresponding cumulative background signal from the Galactic DM halo (resp.

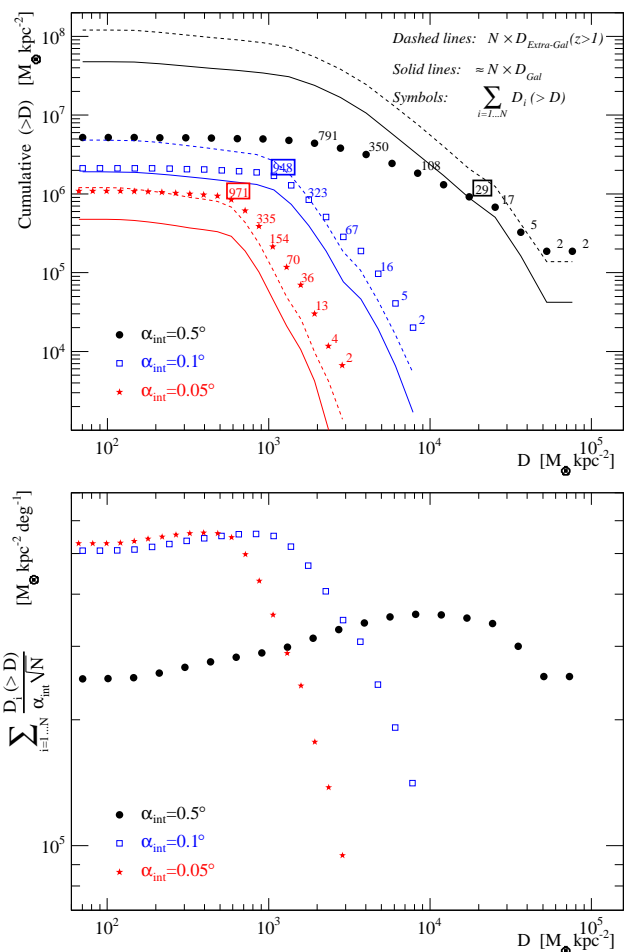


FIG. 3: **Upper panel:** cumulative galaxy cluster signal (solid symbols) and Galactic (solid lines) and extra-galactic upper limit (dashed lines) DM background as a function of  $D$ . The three sets of curves correspond to three different integration angles:  $\alpha_{\text{int}} = 0.5^\circ$  (black circles),  $\alpha_{\text{int}} = 0.1^\circ$  (blue squares), and  $\alpha_{\text{int}} = 0.05^\circ$  (red stars). The number above a given bin corresponds to the total number of clusters with a signal larger than  $D$ . The far left-hand bins contain a total of 1743 clusters. **Bottom panel:** cumulative  $D$  divided by  $\alpha_{\text{int}}\sqrt{N}$ , proportional to the signal-to-noise ratio for a given cluster sample.

extragalactic) is also shown with solid lines (resp. dashed lines). The region between the two lines provides the range of accumulated diffuse DM signal to expect. For 29 clusters, the accumulated background signal from the Galactic DM halo reaches the level of the cluster signal. The integration angle of  $0.5^\circ$ , as used in Fermi-LAT analyses of dwarf spheroidal Galaxies [27, 28], corresponds to the Fermi-LAT angular resolution at around 1 GeV, degrading to  $\sim 1^\circ$  at lower energies and reaching  $0.1^\circ$  above 10 GeV. The blue squares and red stars show the result of repeating the analysis for  $\alpha_{\text{int}} = 0.1^\circ$  and  $0.05^\circ$  respectively (a resolution generally within the capabilities of X-ray instruments, or within reach of the next generation of air-Cerenkov  $\gamma$ -ray telescopes). In these cases the

accumulated Galactic DM plus extra-galactic signal is almost always below the cumulative cluster signal. Because of a smaller integration angle, saturation is not reached at the same cumulated value. For  $\alpha_{\text{int}} = 0.1^\circ$  a gain of a factor  $\sim 100$  in signal is observed between stacking two and 948 sources in the cumulative  $D$ .

The best observational strategy depends not only on the integrated signal and Galactic halo plus extra-galactic DM background, but on the (generally much higher) level of charged particle and diffuse astrophysical gamma-ray backgrounds. In the background-limited regime the best approach is to maximise the signal-to-noise ratio or signal divided by the square-root of background. In the case of uniform background the signal-to-noise is proportional to the cumulative  $D$  divided by  $\alpha_{\text{int}}\sqrt{N}$  (where  $N$  is the number of clusters with  $D_i > D$ ), as shown in the bottom panel of fig. 3. The peaks in these curves (at 29, 948 and 971 clusters for  $\alpha_{\text{int}} = 0.5^\circ$ ,  $0.1^\circ$  and  $0.05^\circ$  respectively) correspond to the optimum stacking approach in the background-limited, rather than signal-limited, regime. With the current MCXC meta-catalogue, there seems to be no advantage in resolutions better than  $0.1^\circ$ . In the signal-limited regime a larger integration angle is preferred. Stacking leads to a signal-to-noise increase of a factor  $\sim 5$ . With a more complete galaxy cluster catalogue, the ‘saturation’ regime (the break seen in the upper-panel curves) would be moved towards smaller  $D$  values and the benefit of the stacking approach could be greater.

#### IV. DISCUSSION AND CONCLUSION

As well as (close to uniform) charged particle backgrounds and the diffuse Galactic DM and astrophysical backgrounds (see e.g. [28]), non-DM gamma-ray emission from galaxy clusters must be considered as another possible source of background and/or confusion [see 29, 30]. No individual galaxy cluster – but for Virgo, for which a gamma-ray emission was detected positionally consistent with the centre of M87 by Fermi-LAT [31] – has been detected in gamma-rays so far, but accelerated particles are expected to provide an additional gamma-ray signal in clusters. Given the present situation of non-detection in the direction of individual massive halos, a stacking analysis is advantageous to place limits on DM decay. Any object for which a signal (of suspected non-DM origin) is observed can be discarded in the analysis at little cost for the exclusion limit. On the other hand, if any signal is observed and is consistent with an astrophysical origin, stacking or merely looking at galaxy clusters will be extremely challenging for DM searches. Alternatively, the strong scaling  $\log N - \log D$  could be a good diagnostic to disentangle a decay from an astrophysical signal if the latter shows a different scaling (Maurin et al., submitted). The case of annihilating DM, which is found to be less favourable but more crucial physically (limits of non-detection are close to the cross-section expected from

that required to match the thermal relic abundance) is discussed in Nezri et al. (in preparation), focusing on the instrumental response of current and future observatories (Fermi and CTA).

To ease further analysis based on our model, we provide with this paper a file containing all the necessary inputs for each cluster. An analysis on real data can certainly be optimised by adapting the integration region for each cluster. Assuming all galaxy clusters share the same DM profile, and given the mass range spanned by the MCXC, we can make the first order approximation that their concentration parameters are the same. In other words, the concentration for an NFW profile is  $c(M) = R_{\text{vir}}/r_s$  and we assume  $c(10^{14}M_\odot) \sim 5$  [25]. Defining

$$\alpha_s \equiv \tan^{-1}\left(\frac{r_s}{d}\right), \quad \alpha_{\text{max}} \equiv \tan^{-1}\left(\frac{5r_s}{d}\right),$$

$$x \equiv \frac{\alpha_{\text{int}}}{\alpha_s}, \quad \text{and} \quad x_{\text{max}} \equiv \frac{\alpha_{\text{max}}}{\alpha_s} \approx 5,$$

we find that there is a universal dependence of the fraction

$$\mathcal{F}_D(x) \equiv \frac{D(x \cdot \alpha_s)}{D_{\text{max}}} \quad (4)$$

on the DM-decay signal. Hence, given  $D(0.1^\circ)$  and  $\alpha_s$  (available in the supplementary file [37], a sample of which being given in table I), and a parametrisation of this universal dependence

$$\mathcal{F}_D(x) = \begin{cases} e^{[-1.17+1.06 \ln(x)-0.17 \ln^2(x)-0.015 \ln^3(x)]} & \text{if } x \leq 5, \\ 1 & \text{otherwise;} \end{cases} \quad (5)$$

the term  $D$  can be calculated for any integration angle, using

$$D(\alpha_{\text{int}}) = D(0.1^\circ) \times \frac{\mathcal{F}_D(\alpha_{\text{int}}/\alpha_s)}{\mathcal{F}_D(0.1^\circ/\alpha_s)}. \quad (6)$$

This parametrisation describing the fraction of the signal in a given angular region is valid down to  $\mathcal{F}_D = 10^{-3}$ . We note that this function is unchanged if an Einasto profile is used, but the  $D$ -values obtained from such a profile are larger than that calculated with an NFW DM distribution.

The values for the ten brightest clusters are given in Table I, with values of  $D$  provided for a  $0.1^\circ$  integration angle (see Supplemental Material [37] for the full list of clusters). We have repeated (not shown) the calculation for  $\alpha_{\text{int}} = 1^\circ$  (an angle for which most clusters fall below the Galactic DM background) to compare the  $D$  factors with those of [8, 13]: our values for Fornax, Coma, AWM 7 and NGC 4636 are found to be lower, but within a factor 2 of what was found in these previous works. In particular, the large difference for the Fornax cluster explains why these authors have flagged it as being the best target for DM decay when it does not make

TABLE I: Ten brightest galaxy clusters (positions taken from the MCXC meta-catalogue [15]) in DM-decay for  $\alpha_{\text{int}} = 0.1^\circ$ .

Name	Index (MCXC)	$l$ (deg)	$b$ (deg)	$d$ (Mpc)	$\alpha_s$ (deg)	$D(0.1^\circ)$ ( $M_\odot \text{ kpc}^{-2}$ )
A426	258	150.6	-13.3	75.0	0.44	$1.0 \cdot 10^4$
Virgo	884	283.8	74.4	15.4	1.09	$1.0 \cdot 10^4$
Coma	943	57.2	88.0	96.2	0.29	$7.3 \cdot 10^3$
Ophiuchus	1304	0.6	9.3	116.	0.27	$7.3 \cdot 10^3$
A3526	915	302.4	21.6	48.1	0.39	$6.8 \cdot 10^3$
A3627	1231	325.3	-7.1	66.0	0.32	$6.5 \cdot 10^3$
AWM7	224	146.3	-15.6	72.1	0.28	$5.7 \cdot 10^3$
A1367	792	235.1	73.0	89.3	0.24	$5.4 \cdot 10^3$
A3571	1048	316.3	28.6	160.	0.18	$5.4 \cdot 10^3$
A2199	1249	62.9	43.7	124.	0.20	$5.1 \cdot 10^3$

it in our top-ten. This is understood as follows. Decay is very sensitive to the mass estimate (which goes directly as the integration of the density). In [8, 13], the authors use  $M_{500}$  values from the HIFLUGCS catalogue [32, 33] that are larger than the ones provided in the MCXC catalogue (e.g., factor of  $\sim 5$ , 2, and 2 for Fornax, Coma, and AMW7 respectively). For the former analyses, the authors used a  $\beta$ -model for the gas distribution [32, 33], whereas the MCXC relies on the more accurate AB-model [34]. As discussed in the App. A of [15], beta-models can produce factor 2 higher, or lower, values of  $M_{500}$ , depending on the core radii used. The masses for the MCXC sample could still suffer from systematics, as for instance from the use of the hydrostatic equilibrium hypothesis. However many comparisons to numerical simulations indicate that these uncertainties

are  $< 15 - 20\%$  [35]. In any case, if the signal from the brightest source is overestimated (resp. underestimated) by a factor  $f$  the improvement factor will increase (resp. decrease) roughly by the same amount. For the MCXC, we recall that  $M_{500}$  and  $R_{500}$  are obtained from the X-ray luminosity, making use of the  $L_X - M_{500}$  scaling relation derived for the REXCESS sample by [36]. The mass estimate not only links to the  $L_X$  measurement, but also to the intrinsic scatter about the scaling relation. Further conversions to  $R_{200}$  may amplify this dispersion effect. This stresses that caution is advised when working with individual clusters for which mass and radius are inferred from the X-ray luminosity. In that respect, stacking provides a more robust approach as it washes out those uncertainties.

To conclude, we have shown that a stacking approach can help to push down by a factor of 5 (for the background-limited regime) to 100 (in the signal-limited case) the current observational limits on decaying DM (when using the MCXC meta-catalogue of galaxy clusters). A more thorough analysis (e.g., using deeper galaxy cluster catalogues and including absorption on the extragalactic background, uncertainties on DM profiles, etc.) is left for future work. Meanwhile, we provide the necessary inputs to apply this idea to existing experiments (for example Fermi-LAT).

## Acknowledgments

We thank the anonymous referee for the constructive criticism that helped clarify the paper. RW is supported by an STFC post-doctoral fellowship.

- 
- [1] F. Takayama and M. Yamaguchi, *Physics Letters B* **485**, 388 (2000), arXiv:hep-ph/0005214.
- [2] W. Buchmüller, L. Covi, K. Hamaguchi, A. Ibarra, and T. T. Yanagida, *Journal of High Energy Physics* **3**, 37 (2007), arXiv:hep-ph/0702184.
- [3] T. Asaka, S. Blanchet, and M. Shaposhnikov, *Physics Letters B* **631**, 151 (2005), arXiv:hep-ph/0503065.
- [4] C.-R. Chen, F. Takahashi, and T. T. Yanagida, *Physics Letters B* **671**, 71 (2009), 0809.0792.
- [5] C. Arina, T. Hambye, A. Ibarra, and C. Weniger, *J. Cosmology Astropart. Phys.* **3**, 24 (2010), 0912.4496.
- [6] M. Pospelov and M. Trott, *Journal of High Energy Physics* **4**, 44 (2009), 0812.0432.
- [7] K. Hamaguchi, S. Shirai, and T. T. Yanagida, *Physics Letters B* **654**, 110 (2007), 0707.2463.
- [8] X. Huang, G. Vertongen, and C. Weniger, *ArXiv e-prints* (2011), 1110.1529.
- [9] A. Boyarsky, O. Ruchayskiy, D. Iakubovskiy, A. V. Maccio', and D. Malyshev, *ArXiv e-prints* (2009), 0911.1774.
- [10] A. Boyarsky, O. Ruchayskiy, D. Iakubovskiy, M. G. Walker, S. Riemer-Sørensen, and S. H. Hansen, *MNRAS* **407**, 1188 (2010), 1001.0644.
- [11] G. Bertone, W. Buchmüller, L. Covi, and A. Ibarra, *J. Cosmology Astropart. Phys.* **11**, 3 (2007), 0709.2299.
- [12] W. B. Atwood, A. A. Abdo, M. Ackermann, W. Althouse, B. Anderson, M. Axelsson, L. Baldini, J. Ballet, D. L. Band, G. Barbiellini, et al., *ApJ* **697**, 1071 (2009), 0902.1089.
- [13] L. Dugger, T. E. Jeltema, and S. Profumo, *J. Cosmology Astropart. Phys.* **12**, 15 (2010), 1009.5988.
- [14] M. Cirelli, P. Panci, and P. D. Serpico, *Nuclear Physics B* **840**, 284 (2010), 0912.0663.
- [15] R. Piffaretti, M. Arnaud, G. W. Pratt, E. Pointecouteau, and J.-B. Melin, *A&A* **534**, A109 (2011), 1007.1916.
- [16] A. Boyarsky, A. Neronov, O. Ruchayskiy, M. Shaposhnikov, and I. Tkachev, *Physical Review Letters* **97**, 261302 (2006), arXiv:astro-ph/0603660.
- [17] L. Zhang, C. Weniger, L. Maccione, J. Redondo, and G. Sigl, *J. Cosmology Astropart. Phys.* **6**, 27 (2010), 0912.4504.

- [18] G. Hütsi, A. Hektor, and M. Raidal, *J. Cosmology Astropart. Phys.* **7**, 8 (2010), 1004.2036.
- [19] I. Cholis, *J. Cosmology Astropart. Phys.* **9**, 7 (2011), 1007.1169.
- [20] J. Ke, M. Luo, L. Wang, and G. Zhu, *Physics Letters B* **698**, 44 (2011), 1101.5878.
- [21] M. Garny, A. Ibarra, D. Tran, and C. Weniger, *J. Cosmology Astropart. Phys.* **1**, 32 (2011), 1011.3786.
- [22] A. Charbonnier, C. Combet, and D. Maurin, *Computer Physics Communications* **183**, 656 (2012).
- [23] V. Springel, J. Wang, M. Vogelsberger, A. Ludlow, A. Jenkins, A. Helmi, J. F. Navarro, C. S. Frenk, and S. D. M. White, *MNRAS* **391**, 1685 (2008), 0809.0898.
- [24] Navarro, Frenk & White, *ApJ* **490**, 493 (1997), astro-ph/9611107.
- [25] A. R. Duffy, J. Schaye, S. T. Kay, and C. Dalla Vecchia, *MNRAS* **390**, L64 (2008), 0804.2486.
- [26] P. Predehl, R. Andritschke, W. Becker, H. Böhringer, W. Bornemann, H. Bräuninger, H. Brunner, M. Brusa, W. Burkert, V. Burwitz, et al., in *Society of Photo-Optical Instrumentation Engineers (SPIE) Conference Series* (2011), vol. 8145 of *Society of Photo-Optical Instrumentation Engineers (SPIE) Conference Series*.
- [27] M. Ackermann et al., *J. Cosmology Astropart. Phys.* **5**, 25 (2010), 1002.2239.
- [28] M. Ackermann et al., *Physical Review Letters* **107**, 241302 (2011), 1108.3546.
- [29] T. E. Jeltema, J. Kehayias, and S. Profumo, *Phys. Rev. D* **80**, 023005 (2009), 0812.0597.
- [30] A. Pinzke, C. Pfrommer, and L. Bergstrom, *ArXiv e-prints* (2011), 1105.3240.
- [31] A. A. Abdo, M. Ackermann, M. Ajello, W. B. Atwood, M. Axelsson, L. Baldini, J. Ballet, G. Barbiellini, D. Bastieri, K. Bechtol, et al., *ApJ* **707**, 55 (2009), 0910.3565.
- [32] Y. Chen, T. H. Reiprich, H. Böhringer, Y. Ikebe, and Y.-Y. Zhang, *A&A* **466**, 805 (2007), arXiv:astro-ph/0702482.
- [33] T. H. Reiprich and H. Böhringer, *ApJ* **567**, 716 (2002), arXiv:astro-ph/0111285.
- [34] G. W. Pratt and M. Arnaud, *A&A* **394**, 375 (2002), arXiv:astro-ph/0207315.
- [35] R. Piffaretti and R. Valdarnini, *A&A* **491**, 71 (2008), 0808.1111.
- [36] G. W. Pratt, J. H. Croston, M. Arnaud, and H. Böhringer, *A&A* **498**, 361 (2009), 0809.3784.
- [37] See Supplemental Material at [enter URL] for the D-values of all MCXC objects.